RJC

RASĀYAN *J. Chem.*
Vol. 17 | No. 3 |752-766| July - September | 2024
ISSN: 0974-1496 | e-ISSN: 0976-0083 | CODEN: RJCABP
http://www.rasayanjournal.com
http://www.rasayanjournal.co.in

COMPUTATIONAL, EXPERIMENTAL SPECTRAL ANALYSIS AND STRUCTURAL PARAMETERS OF 4, 5-DIMETHYL-2-NITRO ANILINE

Bandana Sharma[1,✉] and Munish Kumar Yadav[2]
[1]Department of Applied Sciences & Humanities, Ajay Kumar Garg Engineering College, Ghaziabad-201009, Uttar Pradesh, India
[2]Department of Physics, Deva Nagri College, Meerut-250002-Uttar Pradesh, India
✉Corresponding Author: sharmabandana@akgec.ac.in

ABSTRACT
The infrared and laser Raman spectra of 4, 5-dimethyl-2-nitroaniline were measured and used for experimental spectrum analysis for current work. On a computational level, Hartree-Fock and density functional theory were employed to perform geometry and vibrational spectral analysis. Here, scaled frequencies are displayed in addition to IR, Raman intensities, and decreased masses. Utilizing HF/6-31+G (d, p), HF/6-311++G (d, p), and B3LYP/6-31+G (d, p) approaches, the various thermodynamical parameters are tabulated. These include entropy, enthalpy, and specific heat. The geometrical footprints, such as bond length and bond angles, are further explored in this paper on a computational level.
Keywords: 4,5-Dimethyl-2-Nitro Aniline, Hartree-Fock, Density Functional Theory, IR and Laser Raman Spectra.
RASĀYAN *J. Chem.*, Vol. 17, No.3, 2024

INTRODUCTION

The chemical industry as well as the medical industry depends heavily on aromatic amines. A lot of colours, insecticides, polymers, medicines and antioxidants are made with aniline and its derivatives. Many practical and scientific applications rely on anilines. Anilines are used in the rubber industry to make rubber chemicals and goods including gloves, balloons, and vehicle tires. The use of aniline derivatives in the synthesis of polyurethane, which is essential for the production of plastics, has gained popularity. The global aniline derivatives market is anticipated to expand in the near future due to the increasing need for plastics in the medical sector for the production of medical equipment such as catheters, tubes, masks, and bags. Medical plastics are affordable, lightweight, extremely sterilizable, quickly producible, safe, and chemically resistant. As a result, the demand for anilines and their derivatives has increased substantially.[1,2] The agricultural sector heavily relies on aniline derivatives. They work in the agrochemical industry, making agrochemicals. Thus, the growth of the agricultural sectors in both developed and developing nations is the force that is driving the market for aniline derivatives worldwide. Numerous researchers are interested in the structural and spectral characteristics of aniline because of its wide range of applications.[1-6] In anilines and their derivatives, the amino group is essential for engaging with the proper receptors. The uniformity of the molecule in aniline is influenced by the amino group. Adding another substituent group to aniline causes additional alterations to the molecule's charge distribution, which in turn has an impact on its structural and vibrational properties. The structure and spectrum analysis of aniline and its methyl derivatives are the subject of several experimental and theoretical investigations.[1-6,10,14,17,19-20] The structural details and frequency analyses for 5-nitro-2-flouroaniline and 2-nitro-5-fluoroaniline were published by Ram Kumar and colleagues.[1] The spectrum characteristics of 2,6-dibromo-3-chloro-4-fluoroaniline were investigated by Esme and his colleagues.[2] Yurdakul and coworkers have published the 3-chloro-4-methyl aniline's IR and Raman spectra.[3] Krishna Kumar and his co-workers utilize DFT analysis to examine the vibrational spectra of 2-(methylthio) aniline.[4] Chloro-substituted anilines were subjected to IR, Raman, and DFT calculations by Rai and his associates.[5] In a different investigation, Rai and his colleagues reported the overtone spectra of alkyl-substituted anilines.[6] Experimental methods are essential for the study of aromatic compounds. However, giving a thorough structural interpretation of the results might be rather

challenging.[7] Although computational and experimental methods are sometimes seen as two distinct and independent approaches, there is no denying the strength and utility of merging the two.[8] Numerous researchers conducted HF and DFT spectral assessments for many substituted aniline molecules in conjunction with experimental data.[10-19, 21, 23-24] In the present study, we provide a brief explanation of how the experimental data for 4,5-dimethyl-2-nitro aniline can be integrated with computational techniques (HF and DFT methods). This coupling will help us learn more about the molecular mechanism and broaden the scope of spectral interpretation. According to a review of the literature, there have not yet been any computational evaluations for 45DM2NA described. Thus, with this study, we attempted to obtain the structural characteristics and spectral fingerprints of the 45DM2NA. As a result, the current analysis is designed to thoroughly examine both the experimental and computational vibrational spectra of the aforementioned substituted aniline. HF and density functional theory were used to do quantum chemical simulations on 45DM2NA for that purpose.

EXPERIMENTAL

Details of Experiment

The molecular structure and atom enumeration of 45DM2NA are shown in Fig.-1. In the form of a fine-crystalline powder, the identified chemical, 45DM2NA, was purchased commercially (Sigma-Aldrich, Germany), and it was utilized exactly as supplied. Its stated purity is greater than 99%. The FT-IR spectra have been captured over the 4000-400 cm^{-1} region. The range of the laser Raman spectrum in this study is from 2000 to 50 cm^{-1}. Experimental infrared and laser Raman spectra were recorded at the University Science Instrumentation Centre, Delhi. The Fourier transform infrared spectrum was acquired employing a Perkin-Elmer spectrometer. The Renishaw inVia reflex micro-Raman spectrometer has been utilized to gather the laser Raman spectra. An argon ion laser with a 514 nm wavelength has been utilized to capture Raman spectra. The FT-IR spectra are displayed in Fig.-2, whereas Fig.-3 displays the laser Raman spectra.

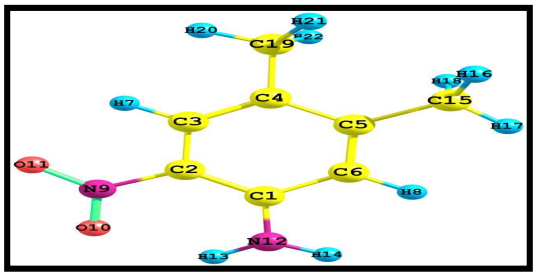

Fig.-1: Atomic Numbering and Structure of 45DM2NA

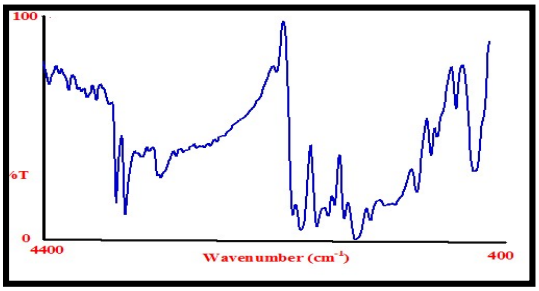

Fig.-2: Experimental FT-IR Spectrum of 45DM2NA in Potassium Bromide Pallets

Details of computation

The structural characteristics for 45DM2NA have been evaluated at the Hartree-Fock and density functional theory levels using the Gaussian 03W program. For the purpose of the discussion in the present paper, levels 1 and 2 are referred to as 6-31+G (d, p) and 6-311++G (d, p), respectively. Geometric investigation as well as estimations of vibrational frequencies at levels 1 and 2 was carried out at the HF level. Furthermore, level 1 DFT calculations were carried out. These computational techniques generate vibrational frequencies along with Raman and infrared intensities. Tables-3, 4, and 5 provide information pertaining to reduced mass and force constant. The 3D GAUSSVIEW visualization tool was used to analyze

the theoretical data. Figures-4 to 9 show the theoretical spectrograms (IR and Raman) that have been built at both the HF and DFT levels.

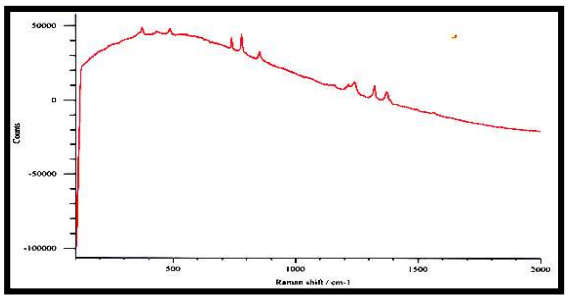

Fig.-3: Laser Raman Spectrum of 45DM2NA

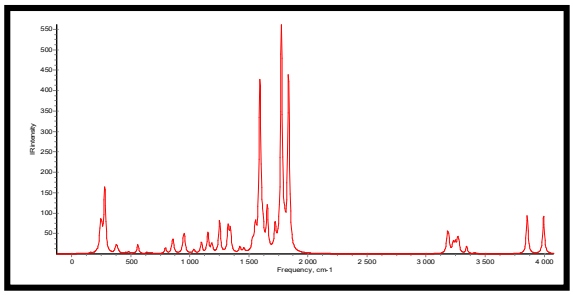

Fig.-4: Theoretical IR Spectrum of 45DM2NA by Hartree-Fock/level 1

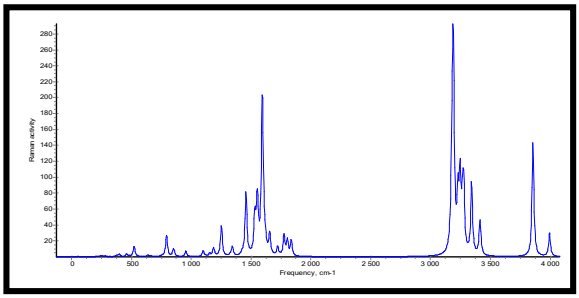

Fig.-5: Theoretical Raman Spectrum of 45DM2NA by Hartree-Fock/level 1

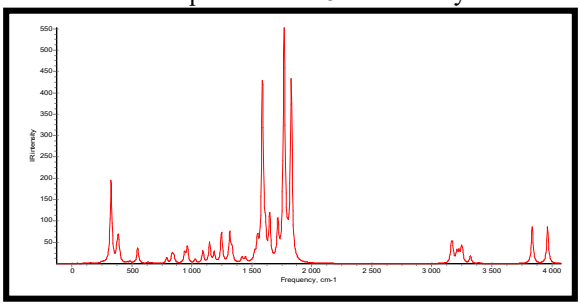

Fig.-6: Theoretical IR Spectrum of 45DM2NA by Hartree-Fock/Level 2

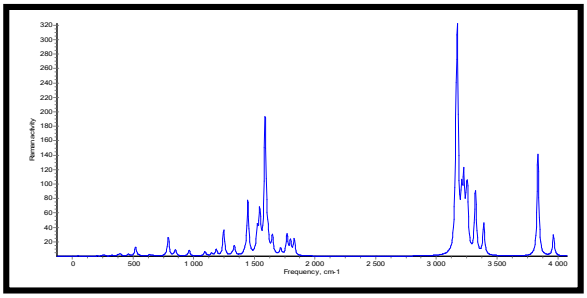

Fig.-7: Theoretical Raman Spectrum of 45DM2NA by Hartree-Fock/Level 2

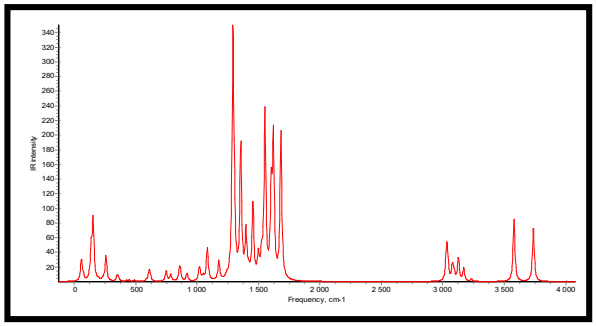

Fig.-8: Theoretical IR Spectrum of 45DM2NA by DFT/Level 1

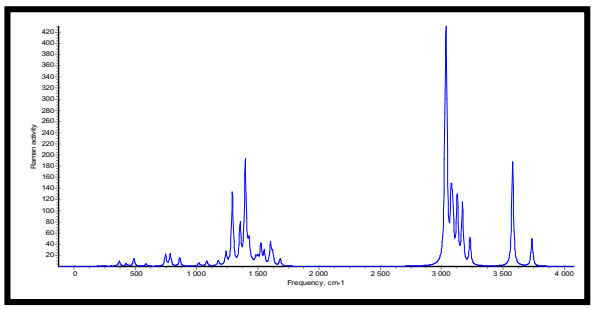

Fig.-9: Theoretical Raman Spectrum of 45DM2NA by DFT/Level 1

Table-1: Experimental Infrared and Raman Frequencies and Assignments for 45DM2NA

IR (cm^{-1})	Raman (cm^{-1})	Assignment	IR (cm^{-1})	Raman (cm^{-1})	Assignment
	160	$\tau(NH_2)$		1260	β(C-H)
	190	γ(C-CH_3), γ(C-NO_2)		1290	β(C-H)
	240	γ(C-NH_2), $\tau(CH_3)$	1310	1321	ν(C- NH_2) , β(C-H)
	290	γ(C-CH_3)	1371	1370	$\nu_s(NO_2)$,$\delta_s(CH_3$)
	340	β(C-CH_3)		1380	$\delta_s(CH_3)$
	380	β(C-NH_2),γ(C-C-C)		1390	$\delta_s(CH_3)$
420	420	β(C-CH_3)		1400	$\delta_{as}(CH_3)$
	430	γ(C-C-C)	1413		ν(C-C), $\delta_{as}(CH_3$)
499	480	γ(C-C-C)		1430	ν(C-C) ,$\delta_{as}(CH_3$)
	510	γ(C-C-C)	1483	1480	ν(C-C) ,$\delta_{as}(CH_3$)
	560	γ(C-C-C)		1530	ν(C-C) ,$\nu_{as}(NO_2)$
	595	β(C-C-C),β(C-NO_2)	1583		ν(C-C) , $\nu_{as}(NO_2)$
610	610	$\rho(NO_2)$, β(C-C-C)	1634	1600	δNH_2, ν(C-C)
728	737	β(C-C-C)	1737		ν(C-C)
766	777	γ(C-H),β(C-C-C),$\omega(NO_2)$	2734		ν_s (CH_3)
853	870	δNO_2, γ(C-H)	2895		ν_s (CH_3)
	900	γ(C-H)	2910		ν_s (CH_3)
	930	ρCH_3),γ(C-H)	2923		ν_{as} (CH_3)
1000		ρCH_3	2990		ν_{as} (CH_3)
1020	1030	ρCH_3	3010		ν(C-H) , ν_{as} (CH_3)
1060		ρCH_3, β(C-H)	3095		ν(C-H) ,ν_{as} (CH_3)
1147	1170	ρCH_3, $t(NH_2)$	3158		ν(C-H)
1190	1190	ν(C-NO_2)	3230		ν(N-H)
1205	1205	ν(C-C),β(C-H) ,ν(C-CH_3)	3372		ν_s (N-H)
1241	1239	ν(C-C) ,ν(C- CH_3)	3487		ν_{as} (N-H)

Where ν–stretching,ν_s-symmetric stretching, ν_{as} -asymmetric stretching, β-in plane bending, γ -out of plane bending, δ-scissoring, δ_s-symmetric bending deformation, δ_{as}-asymmetric bending deformation, ω-wagging, t-twisting, ρ-rocking.

Table-2: Optimized Geometrical Parameters (bond lengths and bond angles) of 45DM2NA using Hartree-Fock/Level 1, Hartee-Fock/Level 2, and DFT/Level 1

Bond Lengths (Å)				Bond angles (degrees)			
Bond	Hartree-Fock		DFT	Bond angles	Hartree-Fock		DFT
	Level 1	Level 2	Level 1		Level 1	Level 2	Level 1
C1-C2	1.399	1.396	1.421	C2-C1-C6	115.8	115.8	116.1
C2-C3	1.404	1.402	1.408	C2-C1-N12	125.9	126.0	124.5
C3-C4	1.367	1.365	1.383	C1-C2-C3	121.0	121.0	120.7
C4-C5	1.418	1.416	1.426	C1-C2-N9	122.1	122.1	122.0
C5-C6	1.371	1.37	1.386	C6-C1-N12	118.3	118.2	119.5
C1-C6	1.413	1.411	1.418	C1-C6-C5	123.3	123.3	123.3
C4-C19	1.511	1.511	1.510	C1-C6-H8	117.4	117.4	117.6
C5-C15	1.509	1.508	1.509	C1-N12-H13	119.8	117.4	119.8
C3-H7	1.072	1.071	1.083	C1-N12-H14	118.1	119.2	119.1
C6-H8	1.076	1.076	1.088	C3-C2-N9	116.9	116.9	117.3
N9-O10	1.205	1.198	1.236	C2-C3-C4	122.3	122.3	122.3
N9-O11	1.196	1.188	1.25	C2-C3-H7	117.4	117.4	117.1
C1-N12	1.356	1.360	1.359	C2-N9-O10	118.6	118.5	118.9
C2-N9	1.441	1.447	1.443	C2-N9-O11	118.4	118.4	118.8
N12-H13	0.991	0.992	1.006	C4-C3-H7	120.2	120.2	120.6
N12-H14	0.992	0.991	1.01	C3-C4-C5	117.6	117.6	118.0
C15-H16	1.085	1.087	1.093	C3-C4-C19	120.9	120.8	120.7
C15-H17	1.083	1.083	1.097	C5-C4-C19	121.5	121.6	121.3
C15-H18	1.085	1.087	1.097	C4-C5-C6	120.0	120.0	119.8
C19-H20	1.083	1.086	1.096	C4-C5-C15	120.3	120.4	120.4
C19-H21	1.086	1.086	1.096	C4-C19-H20	110.5	111.7	110.7
C19-H22	1.086	1.083	1.093	C4-C19-H21	111.7	110.5	111.9
Bond angles (degrees)				C4-C19-H22	111.8	111.7	111.9
Bond angles	Hartree-Fock		DFT				
	Level 1	Level 2	Level 1	C6-C5-C15	119.6	119.6	119.8
H16-C15-H17	108.2	107.7	107.6	C5-C6-H8	119.3	119.3	119.2
H16-C15-H18	107.4	107.4	107.6	C5-C15-H16	110.9	110.8	111.2
H17-C15-H18	108.2	107.7	106.9	C5-C15-H17	111.2	110.8	111.2
H20-C19-H21	107.6	107.4	106.7	C5-C15-H18	110.9	111.2	111.4
H20-C19-H22	107.6	108.2	108	H13-N12-H14	118.6	117.8	121
H21-C19-H22	107.4	108.2	108	O10-N9-O11	122.9	123.1	122.3

Table-3: Computational Thermodynamic Parameters of 45DM2NA

Terms	Total energy	Zero-point energy	Rotational Constants	Dipole Moment	Entropy	Thermal energy	Specific Heat
Units	(a.u.)	(kcal/mol)	(GHz)	(Debyes)	(cal/mol-kelvin)	(kcal/mol))	(cal/mol-kelvin)
HF Level 1	-567.32	117.63	1.67	5.87	Total=102.02 Trans.=41.23 Rot.=30.68 Vib.=30.11	Total=124.48 Trans.=0.89 Rot.=0.89 Vib.=122.70	Total=40.95 Trans.=2.98 Rot.=2.98 Vib.=34.99
HF Level 2	-567.43	117.13	1.67	5.85	Total=102.09 Trans.=41.23 Rot.=30.67 Vib.=30.19	Total=123.96 Trans.=0.89 Rot.=0.89 Vib.=122.18	Total=40.97 Trans.=2.98 Rot.=2.98 Vib.=35.01
DFT Level 1	-570.79	109.52	1.65	5.95	Total=105.46 Trans.=41.23 Rot.=30.72 Vib.=33.51	Total=116.84 Trans.=0.89 Rot.=0.89 Vib.=115.06	Total=43.75 Trans.=2.98 Rot.=2.98 Vib.=37.79

Where trans. stands for translational, rot. for rotational, and vib. for vibration.

Table-4: Vibrational Spectral Characteristics of 45DM2NA using Hartree-Fock/level 1 Computations

S. No.	Wavenumber		IR	Raman		Force
	unscaled	scaled	Intensity	activity	Reduced mass	constant
	(cm^{-1})	(cm^{-1})	(km/mol)	($Å^4$/amu)	(amu)	(mdyne/Å)
1	57	51	1	0	10.66	0.0206
2	97	87	0	0	4.4423	0.0248
3	137	122	0	0	1.0426	0.0115
4	161	143	2	0	2.5604	0.0389
5	208	186	2	0	1.2088	0.0309
6	244	217	58	1	2.8612	0.1005
7	255	227	44	1	3.1279	0.1202
8	281	250	159	1	1.5009	0.0699
9	321	286	0	0	2.5946	0.1578
10	376	334	14	2	4.407	0.3667
11	386	343	12	1	5.4849	0.4808
12	399	355	3	3	4.0767	0.3831
13	461	411	2	3	5.2841	0.663
14	485	431	4	1	3.0748	0.4254
15	523	466	1	13	5.4553	0.8802
16	561	499	22	0	1.0569	0.1961
17	637	567	3	2	3.3399	0.7994
18	662	590	2	1	5.0176	1.2974
19	678	604	2	0	3.9674	1.0757
20	756	673	0	1	3.4734	1.1703
21	794	707	14	27	5.6877	2.1125
22	851	757	16	9	5.1014	2.1771
23	860	765	26	2	11.305	4.9212
24	946	842	27	0	1.4703	0.7751
25	956	850	36	7	5.6363	3.0324
26	1035	921	10	0	1.325	0.8367
27	1099	978	26	7	1.521	1.0818
28	1111	989	0	1	1.5497	1.128
29	1152	1025	7	0	1.4889	1.1643
30	1154	1027	43	3	3.8848	3.0486
31	1172	1043	0	0	1.5636	1.2651
32	1187	1057	22	11	1.6104	1.3371
33	1252	1115	79	38	3.4434	3.1818
34	1325	1179	61	1	2.7548	2.8499
35	1344	1196	53	12	2.6763	2.8466
36	1425	1268	14	3	1.3123	1.5691
37	1458	1297	10	79	4.7846	5.9891
38	1532	1363	23	45	2.2297	3.0825
39	1551	1380	22	54	1.6064	2.2757
40	1557	1386	39	20	1.3955	1.9937
41	1594	1419	422	193	4.0141	6.0107
42	1601	1425	0	15	1.0451	1.5793
43	1615	1438	5	2	1.2613	1.9394
44	1616	1439	17	6	1.0438	1.607
45	1621	1442	32	9	1.2071	1.8677
46	1656	1474	104	26	2.388	3.8582
47	1723	1533	58	11	4.2158	7.3728
48	1776	1581	546	26	3.2997	6.1324
49	1804	1605	31	19	1.8052	3.4596
50	1836	1634	433	20	7.4296	14.7615

51	3179	2829	39	121	1.039	6.1872
52	3191	2840	36	242	1.0378	6.2248
53	3229	2874	24	66	1.1022	6.7699
54	3247	2890	21	88	1.1016	6.8428
55	3267	2908	29	48	1.1006	6.9213
56	3277	2916	19	71	1.1024	6.9742
57	3343	2975	17	90	1.0915	7.1876
58	3413	3038	2	44	1.0924	7.4982
59	3856	3432	94	143	1.046	9.1625
60	3994	3555	93	30	1.1052	10.3877

RESULTS AND DISCUSSION

Experimental Analysis

There will be interactions between the material and the electromagnetic radiation when it is exposed to the radiation. The appealing factor of these interactions is that different aspects of the given material will be revealed by each interaction. There are 60 fundamental vibrational modes produced by 45DM2NA. Of the total 60 vibrations, 41 are within the plane and 19 are outside of it.[18] Table-1 lists the assignments for 45DM2NA based on experimental vibrational analysis. Molecules have a number of bonds with different intensities at different wave numbers that are noticeable within their infrared and Raman spectra. The vibrational characteristics of 45DM2NA are examined using the position, size, and proportional strength of its peaks with respect to chemically related compounds.[14-15,17-18,20-22] Electron-donating groups like methyl groups alter positions 2, 4, and 6 of the benzene ring by rupturing C-H bonds or by boosting electron density through non-resonant mechanisms.[3,10,16-17,20,22] The Methyl group undergoes hyper-conjugation with the surrounding π-systems, whereas the amino group exchanges a single set of electrons to the ring's p-electrons. The molecular orbital approach considers both mechanisms since they include electronic delocalization. Numerous researches on the characteristics of nitro groups have linked their strong tendency to attract electrons via resonance and inductive effects.[1,4,8,10-11,14-17,20] Wherever wavenumbers are mentioned in this section, their units are cm^{-1} for the entire discussion.

Amino Group Vibrations

A doublet is produced by the amino group with a separation of about 70 cm^{-1}.[18] The molecule under examination has one amino group, which is most likely leading to both symmetrical and asymmetrical nitrogen-hydrogen stretching vibrations. These stretching vibrations are identified in the IR spectrum by peaks at 3372 and 3487. The symmetric stretching vibration of nitrogen-hydrogen at 3372 and the asymmetric stretching vibration at 3487 both stand out as exceptionally powerful bands in the infrared spectrum. The NH_2 scissoring mode of the present compound can be seen in the IR spectra at 1634, while its Raman spectra display a very weak band at 1600. The NH_2 twisting mode is responsible for a very weak band at 1170 in the Raman spectra and a medium-strong band at 1147 in the IR spectra. The NH_2 wagging mode of the compound has been identified as a strong band at 610 in the IR spectrum and a weak band at the same frequency in the Raman spectrum. The NH_2 torsion mode has been proposed to be responsible for the weak band that was detected at 160 in the Raman spectrum. Since there is only one amino group, we anticipate a single, powerful C-NH_2 stretching vibration in the 1250–1340 cm^{-1} region.[14, 18, 22] We have two distinct bands in the mentioned region in both the IR and Raman spectra and these two bands are linked to C-NH_2 stretching vibration. According to past investigations, a sharp band in the Raman spectra at 1321 and a medium-strong IR band at 1310 are believed to have the C-NH2 stretching's related characteristics.[4-6,9,13,18] Our current work identifies the C-NH_2 out-of-plane bending as a very faint Raman peak at 240. In-plane bending mode appears as a weak peak at 420 and a medium-strong Raman peak at 380 in the IR spectra.

Methyl Group Vibrations

In this particular investigation, two methyl groups are present at the 4th and 5th locations, as shown in Fig.-1. The molecule resonates in a number of distinct manners as the result of these methyl groups. The FT-IR bands at 3095, 3010, 2990, and 2923 for the molecule mentioned represent the asymmetric stretching

vibration of the methyl. The two FT-IR bands at 2910 and 2895 are credited to the symmetric stretching vibrations of two methyl groups. The title compound's Raman spectra report the symmetric deformation at 1370, 1380, and 1390, and a strong band at 1371 in the IR spectrum is likewise attributed to the same band. The asymmetric bending vibrations of the methyl group have been proposed to be responsible for the bands seen at 1430 and 1480 in the Raman spectra and 1413 and 1483 in the IR spectrum. As indicated in Table 1, these modes overlap with the aromatic stretching vibrations. One methyl group is predicted to have two rocking modes, according to earlier studies.[4,6,14,18-20,22] This causes the bands in the IR spectra at 1000, 1020, and 1060 to be attributed to the methyl group rocking mode. The spikes at 900 and 930 correspond to the methyl group rocking mode. According to previous research, the C-CH_3 stretching seems to be the cause of the strong bands at 1241 and a weak band at 1205.[10,16-17,20] In the Raman spectra, the same stretching vibration appears at 1239 and 1205 C-CH3 out-of-plane bending modes are seen at 180 and 190 within the Raman spectra, while in-plane bending modes are visible at 340 and 420. The CH_3 torsional mode is identified as the weak band at 240 in the Raman spectrum in the current investigation.

Nitro Group Vibrations

A nitro group is present in the second position of the mentioned compound. The most noticeable bands in the spectra of nitro compounds are caused by the nitro-group stretching, which are two significant band wave numbers.[14-17] This is because of their spectral location and powerful intensity. In the mentioned compound, a strong band at 1371 in the IR spectrum and a strong band at 1370 in the Raman spectrum are both indicative of the symmetric NO_2-stretching vibration. The intense signal at 1583 in the infrared range and the medium-strong signal at 1530 within the Raman spectra are generated by the anti-symmetric NO_2-stretching vibration. These vibrations are in excellent agreement with the earlier researchers.[1,4,10] A strong band at 853 in the IR spectra and 870 in the Raman spectra is associated with the NO_2 scissoring mode. The nitro group's wagging state occurs in aromatics at a region in which C and H out-of-plane bending is also active. According to the Raman and IR spectra of 45DM2NA, the wagging mode of the nitro group has been localized at 766 and 777, respectively. NO_2 rocking mode was designated for a peak that appeared at 610 in both the IR and Raman spectra. NO_2 torsion mode for 45DM2NA is missing in both the FT-IR and FT-Raman spectra. Weaker bands are seen in the FT-IR spectra at a few places. These are perceived as overtones or combination bands of the fundamental frequencies.[4,8,17] The stretching of C-NO_2 is seen around 1190 in each of the IR and Raman spectra. The C-NO_2 stretching is present at various places and is combined with other vibrations. C-NO_2 has been observed to bend in and out of a plane in the Raman spectra at 190 and 595, respectively.

Carbon-Carbon and Carbon-Hydrogen Vibrations

Carbon-carbon bonds, specifically carbon-carbon stretching, constitute the majority of bonds in aromatic compounds. This stretching vibration was previously identified by researchers in the range of 1400 to 1650 cm^{-1}.[3-5] As a result, the bands seen at 1480, 1530, and 1600 in the Raman spectra and 1483, 1583, and 1634 in the FTIR are attributed to C-C stretching vibrational modes. In the present work, the aromatic ring is tetra-substituted at positions 1, 2, 4, and 5, leaving only two hydrogen atoms in the third and sixth places. There will therefore be two C-H stretching vibrations as a result of these two hydrogen atoms. The medium-strong bands recorded at 3010, 3095, and 3158 are triggered by the C-H stretching vibrations.[13,18] The Raman spectrum shows no evidence of such vibrations. Previous research investigations indicate that C-H out-of-plane bending arises between 700 and 1000.[5-6] This band is seen in the current investigation at 870 and 900 in the Raman spectra as well as 853 in the IR spectrum. In benzenes between 1350 and 1000, C-H vibrations in-plane bending are regularly noticed. In this instance, this band is given to the frequencies at 1060, 1205, and 1310 in the IR spectrum. The Raman peaks at 1205, 1260, 1290, and 1321 all belong to the same band.

Computational Analysis

Structural Parameters of 45DM2NA

Computational molecular spectroscopy is crucial because molecules have structural information that is stored in their spectra and can only be unlocked using quantum chemistry.[7,23] The marking of the atoms in 45DM2NA is displayed in Fig.-1. Table-2 lists the structure-related parameters that were optimized with

both the HF and DFT approaches in accordance with the atom numbering system. At HF/level 1, the carbon-carbon phenyl ring bond length ranges from 1.367 to 1.418Å. This phenyl C-C bond length extends from 1.365 to 1.416Å at HF/level 2. It indicates that the results at both levels are very congruent and match the lengths of the bonds in molecules of a comparable type.[1,3,10] This bond's length ranges from 1.383 to 1.426Å at the DFT level. The phenyl carbon-carbon bond length of the C4-C5 bond is the longest possible due to both of the methyl groups that are located at the fourth and fifth carbon atoms. At all computational analytical levels, the pattern is the same. Intriguingly, Table 2 shows that the C3-C4 bond is the shortest of all the C-C phenyl bonds. With a value of 1.511Å, the C4-C19 bond length basically remains the same at all three levels. The bond length of the -meta substituent was found to be shorter than that of the -para substituent because the C5-C15 bond length is 1.509, 1.508, and 1.509 Å. Numerous investigations have revealed that substitution has an impact on the C-H bond's length as well. [5-6, 17] In our investigation of the structural characteristics of 45DM2NA, the same phenomenon was also noted. In the mentioned molecule, the NO_2 group is an electron-withdrawn type, whereas the amino and methyl substituents are electron-donating types.[1,3] In benzene, the hydrogen atoms and linked carbon atoms are held together by a sigma bond. In the current study, replacing the hydrogen atom with NO_2 causes a decrease in the electron concentration at the second carbon atom. The C3-H7 bond lengths were computed at the HF level as 1.072 and 1.071Å, respectively, and observed at the DFT level at 1.083Å. The C6-H8 bond length was estimated to be 1.076Å at the HF level and 1.088Å at the B3LYP level, respectively. According to Table-2, the optimized parameters produced by the HF and DFT approaches utilizing various basis sets are roughly comparable to one another. It is noteworthy that N9-O10 and N9-O11 bond lengths varied at each of the three levels of HF and DFT theory. The repulsion between the lone electron pair on the O atom and the electron pair on the nitrogen atom is the reason for this outcome.[14-15,17] There is a slight displacement of nitrogen atoms out of the benzene ring as a result of the interaction between the amino group and aromatic ring. The trends in the deformation of the benzene ring upon replacement, however, are true and consistent with the work of earlier studies.[13,18] The symmetry of the benzene ring is altered with electron-donating and electron-withdrawing substituents at the para locations, resulting in ring angles less than 120°. The C3-C4-C5 bond angle is seen to be 117.6° at both HF levels, whereas it is seen to be 118° at the DFT level. The bond angles for HF/level 1, HF/level 2, and B3LYP/level 1 for C1-C2-C3 are 121, 121, and 120.7°, respectively. The bond angles for the C4-C5-C6 atoms are 120, 120, and 119.8°. Table-2 includes an analysis of all bond lengths and bond angles. At all levels of computational study, the bond angles C1-C6-C5 (123.3°) and C2-C3-C4 (122.3°) have the highest values of the entire C-C-C benzene ring bond angles. The C-C-C bond angle is the smallest for the C2-C1-C6 bond due to the presence of an amino group. At HF levels 1 and 2, it has a value of 115.8°, but at the DFT level, it has a value of 116.1°. Other aniline derivatives, including m-methyl, o-methyl, and p-methyl aniline, are discovered to have similar values.[3,9,10] [20]

Thermodynamic Parameters of 45DM2NA

When conducting the statistical thermodynamic analysis of 45DM2NA, it is assumed that the molecule is at standard pressure and temperature. The contributions spurred on by internal rotations are not taken into account in the computational analysis. At HF, level 1, and level 2, the molecule's zero-point energy from vibration registers at 117.63 and 117.13 Kcal/mol, respectively. The same parameter appears to have a value of 109.52 Kcal/mol at the DFT level. At both HF levels, it is discovered that entropy has a value of almost 102 cal/mol-Kelvin, whereas in the case of DFT, it has a little higher value of 105.5 cal/mol Kelvin. At the DFT level, the specific heat is 43.75 cal/mol-Kelvin, while at HF levels 1 and 2, it is 40.95 cal/mol-Kelvin and 40.97 cal/mol-Kelvin, respectively. At all stages of computational investigation, the value of the rotational constant is discovered to be in close agreement with one another. The computed thermodynamic variables for 45DM2NA, namely entropy, specific heat, thermal energy, rotational constants, and dipole moments, are compiled in Table-3.

Computational Spectral Analysis and Comparison with Experimental Results

Combining experimental data with computational approaches enables us to analyse the results in great depth, which is not possible when utilising simply experimental procedure.[7,23] The outcomes of the experimental and computational procedures are compared after being carried out independently. Results of

computational analysis utilizing HF/level 1, HF/level 2, and DFT/level 1 have been put together and presented in Tables-4, 5, and 6 correspondingly. The experimental results and the frequencies calculated at the theoretical level using various basis sets can be compared, and it emerges that they closely match one another. Table-7 displays an analysis of the experimental spectral outcomes and the computed results. This analysis reveals that the majority of the experimental and computational results are in agreement. We selected a few of the most significant assignments in this section to illustrate our point. Asymmetric and symmetric stretching vibrations are detected at 3487 and 3372, respectively, at the experimental level. At the theoretical levels, asymmetric N-H stretching vibrations are seen at 3555, 3528, and 3587, while symmetric N-H stretching vibrations are seen at 3432, 3414, and 3436. Consistent agreement is also seen between the anticipated NH_2 scissoring, rocking, wagging, and torsional modes and experimental findings. At the experimental level, the vibrations of 3095, 3010, 2990, and 2923 are classified as asymmetric methyl stretching vibrations for the two methyl groups. These stretching vibrations are seen at 2916, 2908, 2890, and 2874 at HF/ level 1, and at 2898, 2889, 2871, and 2855 at HF/ level 2. At 3003, 2999, 2966, and 2954, methyl asymmetric stretching is shown at the DFT/level 1. CH_3 symmetric stretching is seen at 2840 and 2829 at HF/level 1, 2824 and 2814 at HF/level 2, and 2916 and 2908 at DFT/level 1. From the explanation above, it is evident that the expected modes for the methyl groups and experimental results exhibit strong agreement, as shown in Table-7. The benzene ring is surrounded by two hydrogen atoms at the third and sixth places, as can be seen in Fig.-1. Carbon-hydrogen stretching vibrations are produced by these two atoms around the ring. Carbon-hydrogen stretching appears at 3158, 3095, and 3010 at the experimental level. At the computational level, C3-H1 stretching appears at 3038, 3017, and 3102, and C6-H2 stretching is found at 2975, 2956, and 3042. As previously indicated in our work, asymmetric NO_2 stretching vibration is observed at 1583 and 1530. Experimentally, symmetric NO_2 stretching is seen at 1371 and 1370. Theoretically, symmetric NO_2 stretching is associated with vibrations of 1419, 1417, and 1301, whereas asymmetric NO_2 stretching is associated with vibrations of 1634, 1627, and 1490. The deformation vibrations of the NO_2 group have an impact on a number of normal modes in low-frequency region.[1,4] Table-7 lists all additional modes connected to the designated molecule. The theoretically predicted results correlate well with the experimental data.

Table-5: Vibrational Spectral Characteristics of 45DM2NA using Hartree-Fock/level 2 Computations

S. No.	Wavenumber		IR	Raman		Force
	Unscaled	Scaled	Intensity	activity	Reduced mass	constant
	(cm^{-1})	(cm^{-1})	(km/mol)	($Å^4$/amu)	(amu)	(mdyne/Å)
1	50	44	0	1	10.702	0.0155
2	98	87	1	0	4.2201	0.0237
3	134	119	0	0	1.0486	0.011
4	159	142	2	0	2.5094	0.0374
5	207	184	0	0	1.2165	0.0307
6	247	220	3	1	5.0863	0.1835
7	264	235	2	1	3.4658	0.1425
8	320	284	3	0	2.5673	0.1545
9	328	292	195	1	1.3043	0.0825
10	376	335	20	1	4.5858	0.3817
11	387	344	55	1	4.229	0.3733
12	399	355	9	2	3.7449	0.3507
13	462	411	2	3	5.0777	0.6387
14	484	430	4	1	3.0968	0.4266
15	522	464	1	13	5.1025	0.8182
16	550	489	36	1	1.0823	0.1927
17	636	566	3	2	3.3562	0.7993
18	662	589	2	1	4.943	1.2751
19	672	598	1	0	4.0489	1.0777
20	766	682	0	1	3.4318	1.1861
21	791	704	13	26	5.6898	2.0971
22	836	744	21	1	11.229	4.6268

23	851	757	16	8	4.8267	2.0582
24	941	837	24	0	1.4625	0.7627
25	963	857	39	8	6.1027	3.3323
26	1029	916	9	0	1.3225	0.8245
27	1092	972	28	6	1.5659	1.1003
28	1109	987	0	1	1.5515	1.1247
29	1148	1022	18	1	1.8574	1.4423
30	1149	1023	31	3	2.6953	2.0962
31	1169	1040	0	0	1.5689	1.2623
32	1187	1057	24	9	1.601	1.3293
33	1248	1111	71	36	3.1985	2.9343
34	1316	1172	69	2	3.164	3.2301
35	1335	1188	30	13	2.3025	2.4181
36	1419	1263	13	3	1.3066	1.5504
37	1447	1288	12	77	4.7403	5.846
38	1524	1356	16	31	2.0929	2.8636
39	1543	1374	13	42	1.5879	2.2285
40	1549	1379	37	17	1.4687	2.0768
41	1589	1414	428	187	4.4088	6.5595
42	1597	1421	0	12	1.0454	1.5706
43	1610	1433	4	2	1.2465	1.9035
44	1612	1434	17	6	1.0439	1.5972
45	1615	1437	31	9	1.2096	1.8591
46	1649	1468	102	24	2.363	3.7866
47	1717	1528	88	9	4.2502	7.3825
48	1769	1575	538	28	4.1714	7.694
49	1798	1601	24	19	1.5927	3.0347
50	1828	1627	417	22	7.3876	14.55
51	3162	2814	37	132	1.0391	6.1222
52	3174	2824	34	262	1.0378	6.158
53	3208	2855	23	63	1.1019	6.6804
54	3226	2871	23	88	1.1011	6.75
55	3246	2889	29	44	1.1003	6.8321
56	3256	2898	18	67	1.1022	6.8839
57	3322	2956	17	87	1.0915	7.0954
58	3390	3017	2	44	1.0924	7.3957
59	3836	3414	86	142	1.0462	9.0718
60	3964	3528	87	29	1.1046	10.2266

Table-6: Vibrational Spectral Characteristics of 45DM2NA using DFT/level 1 Computations

S.No.	Wavenumber		IR	Raman		
	unscaled	scaled	Intensity	activity	Reduced mass	Force constant
	(cm^{-1})	(cm^{-1})	(km/mol)	($Å^4$/amu)	(amu)	(mdyne/Å)
1	59	57	29	0	6.9672	0.0142
2	73	70	6	0	4.8159	0.0151
3	138	133	38	0	1.3341	0.0150
4	148	143	8	0	1.8354	0.0238
5	155	148	77	0	1.2902	0.0182
6	198	190	3	1	1.2234	0.0281
7	235	225	3	1	5.1699	0.1680
8	259	248	34	1	2.4201	0.0955
9	302	290	0	0	2.5665	0.1377
10	350	336	8	1	4.2814	0.3097
11	361	347	4	0	3.8865	0.2986
12	370	355	0	9	5.7067	0.4606

13	427	410	1	5	5.4514	0.5856
14	450	432	2	0	3.1602	0.3772
15	489	470	2	14	5.6606	0.7981
16	590	566	2	5	3.3676	0.6896
17	611	586	14	0	1.0329	0.2268
18	618	593	1	0	5.1143	1.1497
19	619	594	5	0	3.9599	0.8944
20	680	653	0	0	3.8019	1.0368
21	748	718	7	21	5.7399	1.8908
22	750	720	8	0	11.0605	3.6683
23	786	755	9	22	6.0902	2.2182
24	856	822	13	0	1.4062	0.6076
25	864	829	12	15	4.6084	2.0260
26	919	882	11	0	1.3164	0.6544
27	1018	977	14	4	1.4487	0.8844
28	1025	984	7	3	1.5325	0.9489
29	1050	1008	6	0	1.4498	0.9417
30	1069	1026	0	0	1.5656	1.0540
31	1080	1037	12	2	2.2071	1.5167
32	1084	1041	35	8	2.1243	1.4710
33	1177	1129	26	10	3.4116	2.7825
34	1240	1191	3	23	2.0322	1.8417
35	1292	1240	338	132	4.4531	4.3796
36	1304	1252	41	1	1.4304	1.4338
37	1355	1301	182	71	7.3573	7.9616
38	1397	1341	63	185	5.2312	6.0185
39	1418	1361	10	10	1.2698	1.5043
40	1429	1372	2	36	1.2607	1.5173
41	1454	1396	104	5	2.8391	3.5362
42	1482	1423	0	12	1.0445	1.3520
43	1494	1434	5	1	1.2594	1.6563
44	1498	1438	19	6	1.0430	1.3795
45	1501	1441	9	6	1.2455	1.6542
46	1525	1464	29	37	2.4247	3.3231
47	1552	1490	228	24	4.9005	6.9557
48	1603	1539	113	39	3.7630	5.6983
49	1621	1556	184	21	1.8189	2.8149
50	1682	1615	201	13	6.6149	11.0310
51	3029	2908	38	215	1.0389	5.6174
52	3038	2916	27	302	1.0379	5.6425
53	3077	2954	20	101	1.1005	6.1400
54	3090	2966	11	83	1.0999	6.1865
55	3124	2999	20	43	1.0993	6.3227
56	3128	3003	12	79	1.1009	6.3464
57	3169	3042	18	107	1.0900	6.4498
58	3231	3102	3	47	1.0906	6.7075
59	3579	3436	88	194	1.0471	7.9008
60	3736	3587	75	51	1.1036	9.0779

Table-7: Comparison of Experimental and Computational Vibrational Assignments

Experimental		Computational			Assignment
FT-IR	FT-Raman	Hartree-Fock		DFT	
		Level 1	Level 2	Level 1	
		51	44	57	$\tau(NO_2)$, $\rho(CH_3)$
		87	87	70	$\tau(CH_3)$

		122	119	133	$\tau(CH_3)$
		143	142	143	$\tau(CH_3)$
	160			148	$\tau(NH_2)$
		186	184	190	$\tau(CH_3)$
	190				$\gamma(C\text{-}CH_3),\gamma(C\text{-}NO_2)$
		217	220		$\tau(NH_2)$, $\beta(C\text{-}CH_3)$
		227	235	225	$\tau(CH_3)$
	240	250	284	248	$\tau(CH_3),\gamma(C\text{-}NH_2)$
		286	292	290	$\beta(C\text{-}CH_3)$, $\tau(NH_2)$
	290	334	335	336	$\gamma(C\text{-}CH_3)$
	340				$\beta(C\text{-}CH_3)$
		343	344	347	$\beta(C\text{-}NH_2)$
		355	355	355	$\beta(C\text{-}CH_3)$
	380				$\beta(C\text{-}NH_2)$, $\gamma(C\text{-}C\text{-}C)$
		411	411	410	$\rho(NO_2)$
420	420				$\beta(C\text{-}CH_3)$
	430	431	430	432	$\gamma(C\text{-}H)$, $\gamma(C\text{-}C\text{-}C)$
		466	464	470	$\nu\ (C\text{-}CH_3)$
499	480				$\gamma(C\text{-}C\text{-}C)$
		499	489	566	$\omega\ (NH_2)$
		567	566	586	$\gamma(C\text{-}H)$, $\gamma(C\text{-}CH_3)$
	560				$\gamma(C\text{-}C\text{-}C)$
	595	590	589	593	$\beta(C\text{-}H),\beta(C\text{-}CH_3)$
		604	598	594	$\beta(C\text{-}C\text{-}C)$, $\beta(C\text{-}CH_3)$
610	610				$\rho(NO_2)$
		673	682	653	$\gamma(C\text{-}H)$
728	737	707	704	718	$\beta(C\text{-}C\text{-}C)$
		757			$\beta(C\text{-}H)$, $\nu(C\text{-}CH_3)$
766	777	765	744	720	$\omega(NO_2)$
			757	755	$\gamma(C\text{-}H)$, $\beta(C\text{-}C\text{-}C)$, $\nu(C\text{-}CH_3)$, $\delta(NO_2)$
		842	837	822	$\gamma(C\text{-}H)$
853		850	857	829	$\gamma(C\text{-}H)$, $\delta(NO_2)$
	870				$\gamma(C\text{-}H)$, $\delta(NO_2)$
	900				$\gamma(C\text{-}H)$
	930	921	916	882	$\gamma(C\text{-}H)$, $\rho(CH_3)$
		978	972	977	$\rho(CH_3)$
		989	987	984	$\rho(CH_3)$, $t(NH_2)$
1000					$\rho(CH_3)$, tri. bending
1020	1030	1025	1022	1008	$\rho(CH_3)$, $\gamma(C\text{-}H)$
		1027	1023	1026	$\rho(CH_3)$
		1043	1040	1037	$\rho(CH_3)$, $t(NH_2)$
1060		1057	1057	1041	$t(NH_2\ )$, $\beta(C\text{-}H)$
		1115	1111	1129	$\beta(C\text{-}C\text{-}C)$
1147	1170				$t(NH_2\ )$
1190	1190	1179	1172	1191	$\nu(C\text{-}C)$, $\beta(C\text{-}H)$
1241	1239	1196	1188	1240	$\nu(C\text{-}C)$
	1260	1268	1263	1255	$\beta(C\text{-}H)$
		1297	1288	1301	$\nu(C\text{-}C)$
				1301	$\nu_s(NO_2)$
1310	1321				$\beta(C\text{-}H)$
		1363	1356	1341	$\delta_s(CH_3)$
1371	1370	1380	1374	1361	$\delta_s(CH_3)$, $\nu_s(NO_2)$
	1380	1386	1379	1372	$\delta_{as}(CH_3)$
	1390				$\delta_s(CH_3)$

1413	1400			1396	$\delta_{as}(CH_3)$, $\nu_s(NO_2)$
		1419	1414		$\nu_s(NO_2)$
	1430	1425	1421	1423	$\delta_{as}(CH_3)$, ν(C-C)
		1438	1433	1434	$\delta_{as}(CH_3)$
		1439	1434	1438	$\delta_{as}(CH_3)$
		1442	1437	1441	ν(C-C), $\delta_{as}(CH_3$)
1483	1480	1474	1468	1464	δCH_3, β(C-H)
	1530	1533	1528	1490	ν(C-C), $\nu_{as}(NO_2)$
1583		1581	1575	1539	$\delta(NH_2)$, ν(C-C)
1634	1600	1605	1601	1556	$\delta(NH_2)$
1737		1634	1627	1615	β(C-H), β(C-C-C), $_{as}(NO_2)$
2734		2829	2814	2908	$\nu_s(CH_3)$
2895		2840	2824	2916	$\nu_s(CH_3)$
2910		2874	2855	2954	$\nu_{as}(CH_3)$
2923		2890	2871	2966	$\nu_{as}(CH_3)$
2990		2908	2889	2999	$\nu_{as}(CH_3)$
3010		2916	2898	3003	$\nu_{as}(CH_3)$
3095		2975	2956	3042	ν(C-H)
3158		3038	3017	3102	ν(C-H)
3230					ν_s(N-H)
3372		3432	3414	3436	ν_s(N-H)
3487		3555	3528	3587	ν_{as}(N-H)

CONCLUSION

This work investigates 45DM2NA using computational techniques that reproduce experimental spectra, providing atomic-level descriptions not possible with experimental data. The experimental IR and Raman spectra align with related studies, providing a comprehensive understanding. The study uses HF and DFT analysis for structural specification, revealing exceptional equilibrium geometry performance for bond lengths and angles, and exploring the impact of functional group type on structural features. The study conducted three levels of computational spectral analysis, revealing compatibility between experimental results and vibrational frequency analysis using HF and DFT methods, with both data and models correlating and supporting each other. The thermodynamic parameters, including entropy and specific heat, are computed at three independent levels and the results are compiled.

ACKNOWLEDGEMENTS

The Department of Applied Sciences & Humanities, Ajay Kumar Garg Engineering College, Ghaziabad, India, and the Department of Physics at Deva Nagri College, Meerut, India, are acknowledged by the authors for their assistance in carrying out this study and completing this investigation.

CONFLICT OF INTERESTS

The authors declare that there is no conflict of interest.

AUTHOR CONTRIBUTIONS

All the authors contributed significantly to this manuscript, participated in reviewing/editing, and approved the final draft for publication. The research profile of the authors can be verified from their ORCID IDs, given below:

Bandana Sharma https://orcid.org/0000-0002-8401-1254
Munish Kumar Yadav https://orcid.org/0000-0003-1540-9733

REFERENCES

1. A. R. Kumar, S. Selvaraj, P. Anthoniammal, R. J. Ramalingam, B. Ranjith, P. Jayaprakash and G. P. S. Mol, *Journal of Fluorine Chemistry*, **270**, 110167(2023), https://doi.org/10.1016/j.jfluchem.2023.110167
2. A. Eşme and S. Sağdınç, *Journal of Applied Spectroscopy*, **84**, 1098(2018), https://doi.org/10.1007/s10812-018-0594-8
3. M. Kurt, M. Yurdakul and Ş. Yurdakul, *Journal of Molecular Structure-theochem*, **711**, 25(2004), https://doi.org/10.1016/j.theochem.2004.07.034
4. V. Krishnakumar and V. Balachandran, *Spectrochimica Acta Part A: Molecular and Biomolecular Spectroscopy*, **61**, 1811(2005), https://doi.org/10.1016/j.saa.2004.07.012
5. A. Kumar, S. Kumar and A. Rai, *Vibrational Spectroscopy*, **42**, 397(2006), https://doi.org/10.1016/j.vibspec.2006.05.033
6. V. Kumar, A. Rai, D. K. Rai and S. B. Rai, *Spectrochimica Acta Part A: Molecular and Biomolecular Spectroscopy*, **60**, 53(2004), https://doi.org/10.1016/S1386-1425(03)00179-3
7. F. Wang, *Physical Chemistry Chemical Physics*, **25**, 7090(2023), https://doi.org/10.1039/d3cp00192j
8. A. Kumer, B. Ahmed, A. Sharif and A. Al-Mamun, *Asian Journal of Physical and Chemical Sciences*, **4**, 1(2017), https://doi.org/10.9734/ajopacs/2017/38092
9. E. S. Ashlin, G. E. Sheela and P. R. Babila, *Chemical Physics Impact*, **6**, 100186(2023), https://doi.org/10.1016/j.chphi.2023.100186
10. J. S. John, D. Sajan, P. Prabukanthan, R. Philip and N. Joy, *Optics and Laser Technology*, **113**, 416(2019), https://doi.org/10.1016/j.optlastec.2019.01.014
11. S. Saravanan, A. Sankar and K. Parimala, *Journal of Molecular Structure*, **1127**, 784(2017), https://doi.org/10.1016/j.molstruc.2016.03.018
12. M. Farasat, S. Shojaei, M. M. Golzan and K. Farhadi, *Journal of Molecular Structure*, **1108**, 341(2016), https://doi.org/10.1016/j.molstruc.2015.12.044
13. S. Jeyavijayan and M. Arivazhagan, *Spectrochimica Acta Part A: Molecular and Biomolecular Spectroscopy*, **81**, 466(2011), https://doi.org/10.1016/j.saa.2011.06.039
14. Ü. Ceylan, G. Ö. Tarı, H. Gökçe and E. Ağar, *Journal of Molecular Structure*, **1110**, 1(2016), https://doi.org/10.1016/j.molstruc.2016.01.019
15. S. Thangarasu, V. Siva, S. Kannan, S. A. Bahadur and S. Athimoolam, *Polycyclic Aromatic Compounds*, **43**, 7164(2022), https://doi.org/10.1080/10406638.2022.2130374
16. S. Saravanan, V. Balachandran and K. Viswanathan, *Spectrochimica Acta Part A: Molecular and Biomolecular Spectroscopy*, **121**, 685(2014), https://doi.org/10.1016/j.saa.2013.12.010
17. J. Hernández-Paredes, O. Hernández-Negrete, R. C. Carrillo-Torres, R. Sánchez-Zeferino, A. Duarte-Möller and E. Álvarez, *Spectrochimica Acta Part A: Molecular and Biomolecular Spectroscopy*, **149**, 240(2015), https://doi.org/10.1016/j.saa.2015.04.080
18. B. Sharma, M. K.Yadav and S. Prakash, *Rasayan Journal of Chemistry*, **16**, 905(2023), https://doi.org/10.31788/RJC.2023.1628371
19. M. Anjalin, N. Kanagathara and A. Suganthi, *Materials Today: Proceedings*, **33**, 4751(2020), https://doi.org/10.1016/j.matpr.2020.08.358
20. J. K. Ojha, B. V. Reddy and G. R. Rao, *Spectrochimica Acta Part A: Molecular and Biomolecular Spectroscopy*, **96**, 632(2012), https://doi.org/10.1016/j.saa.2012.06.035
21. V. Balachandran, G. Santhi, V. Karpagam and A. B. Lakshmi, *Journal of Molecular Structure*, **1047**, 249(2013), https://doi.org/10.1016/j.molstruc.2013.05.021
22. P. Manjusha, J. C. Prasana, S. Muthu and B. F. Rizwana, *Computational Biology and Chemistry*, **88**, 107330(2020), https://doi.org/10.1016/j.compbiolchem.2020.107330
23. F. Wang, *Physical Chemistry Chemical Physics*, **25**, 7090(2023), https://doi.org/10.1039/d3cp00192j
24. P. Thamizhini, A. Sharmila and K. Lakshmi Prabha, *Rasayan Journal of Chemistry*,**14**, 288(2021), https://doi.org/10.31788/rjc.2021.1415890

[RJC- 8865/2024]